Biogeochemistry
https://doi.org/10.1007/s10533-023-01045-8

ORIGINAL RESEARCH ARTICLE

Coarse woody debris accelerates the decomposition of deadwood inputs across temperate forest

Mark A. Bradford · G. F. Ciska Veen · Ella M. Bradford · Kristofer R. Covey · Thomas W. Crowther · Nicholas Fields · Paul T. Frankson · Javier González-Rivero · Fiona V. Jevon · Sara E. Kuebbing · Steven McBride · Jacqueline E. Mohan · Emily E. Oldfield · Angela M. Oliverio · Alexander Polussa · Corinna Steinrueck · Michael S. Strickland · Elisabeth B. Ward · Carl Wepking · Daniel S. Maynard

Received: 2 June 2022 / Accepted: 1 May 2023

Abstract Wood decomposition is regulated by multiple controls, including climate and wood traits, that vary at local to regional scales. Yet decomposition rates differ dramatically when these controls do not. Fungal community dynamics are often invoked to explain these differences, suggesting that knowledge of ecosystem properties that influence fungal communities will improve understanding and projection of wood decomposition. We hypothesize that deadwood inputs decompose faster in forests with higher stocks of downed coarse woody material (CWM) because CWM is a resource from which lignocellulolytic fungi rapidly colonize new inputs. To test this hypothesis, we measure decomposition of 1,116 pieces of fine woody material (FWM) of five species, incubated for 13 to 49 months at five locations spanning 10°-latitude in eastern U.S. forest. We place FWM pieces near and far from CWM across observational transects and experimental common gardens. Soil temperature positively affects location-level mean decomposition rates, but these among-location differences are smaller than within-location variation in decomposition. Some of this variability is

Responsible Editor: Kate Lajtha

Supplementary Information The online version contains supplementary material available at https://doi.org/10.1007/s10533-023-01045-8.

M. A. Bradford (✉) · E. M. Bradford · N. Fields · J. González-Rivero · F. V. Jevon · S. E. Kuebbing · A. Polussa · E. B. Ward
The Forest School, Yale School of the Environment, Yale University, New Haven, CT 06511, USA
e-mail: mark.bradford@yale.edu

G. F. C. Veen
Department of Terrestrial Ecology, Netherlands Institute of Ecology, PO Box 50, 6700AB Wageningen, The Netherlands

K. R. Covey
Environmental Studies and Sciences, Skidmore College, Saratoga Springs, NY 12866, USA

T. W. Crowther · D. S. Maynard
Institute of Integrative Biology, ETH Zurich, Univeritätstrasse 16, 8006 Zurich, Switzerland

P. T. Frankson · J. E. Mohan
Odum School of Ecology, University of Georgia, Athens, GA 30601, USA

S. McBride
Department of Plant and Soil Science, University of Kentucky, Lexington, KY 40546, USA

E. E. Oldfield
Environmental Defense Fund, Washington, DC 20009, USA

A. M. Oliverio
Department of Biology, Syracuse University, 107 College Place, Syracuse, NY 13210, USA

C. Steinrueck
Warren Wilson College, 701 Warren Wilson Rd, Swannanoa, NC 28778, USA

Published online: 08 May 2023

caused by CWM, where FWM pieces next to CWM decompose more rapidly. These effects are greater with time of incubation and lower initial wood density of FWM. The effect size of CWM is of the same relative magnitude as for the known controls of temperature, deadwood density and diameter. Abundance data for CWM is available for many forests and hence may be an ecosystem variable amenable for inclusion in decomposition models. Our findings suggest that conservation efforts to rebuild depleted CWM stocks in temperate forests may accelerate decomposition of fresh deadwood inputs.

Keywords Basidiomycetes · Carbon cycling · Downed deadwood · Ecosystem controls · Scale · Wood-rot fungi

Introduction

A critical determinant of the carbon (C) balance of forests is the turnover rate of deadwood (Harris et al. 2021). Representing 73 ± 6 Pg C globally, which is ~ 17% of the total wood carbon in the world's forests, deadwood is a substantial C stock (Jia-bing et al. 2005; Weedon et al. 2009; Pan et al. 2011). The decomposition of this stock is a key intermediary step in the conversion of live tree biomass to soil organic C, the two largest C stocks in forests (Heath et al. 2003; EPA 2013). Yet how the decomposition rate of deadwood is controlled remains highly uncertain (Keenan et al. 2013). Such uncertainty compromises the reliability of global and regional C-cycle model projections (Yin 1999; Zell et al. 2009; Pugh et al. 2019), as well as our ability to anticipate the effects of environmental change on forest ecosystems (Cornwell et al. 2009) because deadwood is a hotspot for nitrogen (N) accumulation and key habitat for many species of animals, plants and microbes (Lindenmayer et al. 2002; Harmon et al. 2004; Stokland et al. 2012). Understanding the controls on wood decomposition can instrumentally inform how stocks of deadwood should be managed to sustain forest nutrient supplies, biodiversity, productivity and C storage (Lindenmayer et al. 2002; Edman et al. 2004; Olsson et al. 2011; Harmon et al. 2020).

Many C cycle models assume that decomposition rates of deadwood at regional-to-global scales are mainly a function of climate (Oleson et al. 2013). Empirical studies show that wood decomposition rates at these scales are also strongly controlled by the traits of deadwood (e.g., initial wood density), as well as its size and orientation (e.g., whether standing or downed) (Weedon et al. 2009; Freschet et al. 2012; Jackson et al. 2013; Bradford et al. 2021). Yet decomposition rates can vary to the same extent locally as they do regionally even when deadwood traits, size and orientation are the same (Boddy and Swift 1984; Boddy et al. 1989; Bradford et al. 2014, 2021). The primary factor invoked to explain such dramatic local-scale differences in decomposition rates, at least in temperate forests, is the composition of the fungal community that colonizes deadwood (Boddy and Swift 1984; van der Wal et al. 2015; Smith and Peay 2021). This conclusion is consistent with myriad experimental and observational studies, suggesting the prominent role of fungal-life history strategies, functional trait expression and competitive interactions in governing wood decomposition rates at local scales (Toljander et al. 2006; Fukami et al. 2010; Dickie et al. 2012; Smith and Peay 2021). One potential way to reduce the uncertainty associated with projecting wood decomposition rates may be to identify ecosystem properties that affect fungal colonization of deadwood and then quantify their influence on decomposition rates at regional scales.

The abundance and distribution of downed, coarse woody material (CWM) in forest understories is an ecosystem property that might cause differences in decomposition rates because it serves as a source of wood decomposers such as basidiomycete fungi capable of brown- and white-rot decay. These fungi are considered primary agents of wood decomposition (Boddy et al. 2008; van der Wal et al. 2015). Of importance are lignocellulolytic basidiomycetes that aggregate their hyphae into thick mycelial cords or rhizomorphs (Crowther et al. 2014). These hyphal-aggregating fungi are referred to as "non-unit restricted fungi" because their mycelia can extend from their existing substrates to access discrete wood resources. This ability to forage across the soil-litter interface and connect discrete pieces of deadwood, combines with their ability to translocate water,

M. S. Strickland
Department of Soil & Water Systems, University of Idaho, Moscow, ID 83844, USA

C. Wepking
Department of Biological Sciences, Virginia Tech University, Blacksburg, VA 24061, USA

nutrients and C among this resource network (Cairney 2005). These abilities confer a strong competitive advantage to non-unit restricted fungi because they can leverage their high abundances and abilities to redistribute energy and nutrients from one piece of deadwood to rapidly colonize fresh deadwood inputs. As such, non-unit restricted fungi often outcompete other wood-rot fungi (Boddy 2000; Crowther et al. 2014) and facilitate rapid decomposition of the fine and CWM classes in which they predominate (Thompson and Rayner 1983; Coates and Rayner 1985). However, foraging of these lignocellulolytic fungi is likely to be maximal nearer (e.g., < 1 m) to CWM because invertebrate grazing, such as by isopods and millipedes, increasingly limits fungal foraging with greater distance from CWM (Crowther et al. 2011). The abundance and distribution of CWM may then be a key ecosystem property influencing the decomposition rates of deadwood inputs. If found to be the case, such knowledge could be immediately leveraged to more confidently project wood decomposition rates given the availability of national datasets on CWM stocks (Woodall et al. 2013; Wilson et al. 2013).

We hypothesized that decomposition of new deadwood inputs is faster when they are adjacent to, as opposed to away from, downed CWM because wood-rot fungi rapidly colonize and decompose the proximal resource. As well as foraging by non-unit restricted fungi, more rapid colonization adjacent to CWM might also occur via spores and fragments of hyphae dispersed, for example, by animals such as beetles (Edman et al. 2004; Olsson et al. 2011). We do not attempt to resolve these different colonization mechanisms but do attempt to separate them from other mechanisms of CWM effects such as modification of the microclimate and soil nutrient availability (Harmon et al. 2004; Edman et al. 2004; Hafner et al. 2005; Olsson et al. 2011). To test the colonization hypothesis, we established study plots at five locations, spanning a mean soil temperature gradient of ~ 10 ℃, in eastern U.S. temperate, mixed forest. We then followed the decomposition of pieces of freshly cut boles from saplings of five tree species which differed in their initial wood traits. We used a structural causal modeling approach to estimate the effect size of CWM proximity on decomposition rates and to explore the potential for different causal pathways to explain our results. We find that proximity to downed CWM accelerates the decomposition of fresh deadwood inputs and that the alternate causal pathways did not account for the observed effects. Our study reinforces the expectation that local conditions which promote fungal colonization accelerate wood decomposition rates and situates this knowledge in a broader spatial context, whereby ecosystem properties influencing these fungi exert control on wood decomposition rates at regional scales.

Methods

Study locations and design

We worked at five locations which were, from north to south: (1) Hubbard Brook Experimental Forest (HBR), New Hampshire; (2) Yale-Myers Forest (YMF), Connecticut; (3) Mountain Lake Biological Station (MLB), Virginia; (4) Coweeta Hydrologic Laboratory (CWT), North Carolina; and (5) Whitehall Experimental Forest (WHF), Georgia. The locations spanned a regional climate gradient, with variation in macroclimate generated by latitudinal and elevational differences among the locations (Table S1). The stands in which we established our work at each location were dominated by *Quercus-Carya* (i.e., oak-hickory) overstory species at the four most southerly locations, and by *Fagus-Acer-Betula* (i.e., beech-maple-birch) at the most northerly location. All stands were second growth, which dominate eastern U.S. temperate forests, and the stand ages (80–100 years old) provided ample time for the accrual of dead wood. Table S1 provides further details on location geography and ecosystem characteristics.

At each location in May 2016, we established observational transects and experimental common gardens. In each we followed the decomposition of pieces of freshly cut boles from saplings of five tree species, both next to and distant from CWM. The freshly cut boles had dimensions consistent with the diameter definition for large fine-woody debris (FWM: 2.54 to 7.6 cm dia.) and narrow pieces of CWM (i.e., dia. > 7.6 cm) (Woodall and Monleon 2008). We describe their preparation in Sect. "FWM pieces" and, given their narrow diameter (ranging from 3.5 to 8.0 cm) and short length (i.e., 10 cm), refer to them going forward as FWM pieces.

The observational transects consisted of a 140-m transect (or two transects summing to 140 m) that ran from the toe of a slope to the ridge to capture variation in microclimate, particularly moisture availability given its importance as a control on decomposition rates (Dix 1985; Lustenhouwer et al. 2020). Every 10 m, starting at 0 m on the transect (and hence at 15 points along the transect), one FWM piece of each of the five species was placed end-on-end (each piece 5 cm apart) running parallel to a naturally occurring, downed tree bole (Fig. S1) that either crossed the transect or was the nearest observable perpendicular to the transect position. We only placed FWM pieces next to downed wood if it met criteria for the definition of CWM following Woodall and Monleon (2008), where the downed wood was greater than 7.6 cm in dia. and more than 1-m long. Further, the downed wood had to be in decomposition stages II to IV (Waddell 2002), which are the dominant decomposition stages in eastern U.S. forests (Woodall et al. 2013). A second set of FWM pieces was organized similarly but at least 5 m away from downed CWM. Cords and other hyphal aggregations of non-unit restricted fungi can potentially forage tens of meters but are presumed most abundant proximal to the deadwood source they colonized (Thompson and Rayner 1982, 1983).

Overall, the observational transect design involved placing 30 FWM pieces per species and therefore 150 FWM pieces total per location (750 FWM pieces across all locations: 15 microsite patches per transect × 2 CWM positions × 5 species × 5 locations). FWM pieces were placed flush with the litter layer and in contact with the surface soil. The short length of the FWM pieces (i.e., 10 cm) ensured that the entire underside of the FWM piece was in contact with the soil, permitting even access along the piece to the soil surface and hence a more standard microsite environment. The design ensured that no FWM pieces sat above the soil because such aerial placement can severely limit wood moisture and hence fungal-mediated decomposition (Bradford et al. 2021).

Common gardens consisted of six 25-m^2 (5 × 5 m) plots in a paired design at each location. Gardens were established along the same slope as the observational transects to capture microclimate variation, with one pair of gardens at the toe, mid and top (i.e., ridge) of the slope. In each pair of gardens, CWM was manipulated to create zero versus high-density downed CWM (Fig. S2). Specifically, natural CWM in decay classes II to IV (and of approximately equal volumetric proportions) was collected adjacent to the transects and aggregated to create the high-density CWM gardens. We selected garden locations with minimal-to-no current CWM, to avoid selecting gardens already containing elevated abundances of hyphal biomass of wood-rot fungi. Gardens were periodically checked to remove any deadwood that fell into them across the course of the study.

FWM pieces of two of the species (i.e., red maple and eastern white pine) were placed in four microsites within each common garden. In the high-density CWM gardens, FWM pieces were placed immediately adjacent to downed CWM. A single maple and pine piece was placed in each garden microsite, and all FWM pieces were placed following the same spacing and soil-contact protocol as for the observational transects. At each common garden there were then 8 FWM pieces, and with three garden pairs per location, there were 24 FWM pieces per tree species and 48 total per location (yielding 240 FWM pieces total across the five locations). At the YMF location, we placed additional maple and pine FWM pieces in each microsite and harvested one of each species per microsite at 13 and 49, as well as 25, months after garden establishment.

FWM pieces

We used wood from five tree species which differ in trait values in ways that influence decomposition rates, such as wood density, initial N content and secondary chemicals (Weedon et al. 2009; Russell et al. 2014). The species were: (1) northern red oak: *Quercus rubra* L.; (2) American beech: *Fagus grandifolia* Ehrh.; (3) black or sweet birch: *Betula lenta* L.; (4) red maple: *Acer rubrum* L.; and (5) eastern white pine, *Pinus strobus* L. These species are representative of common overstory species, that occur across the geographic range encapsulated by the locations and differ by growth habit (i.e., broadleaf, deciduous hardwood vs. needle, evergreen, softwood), mycorrhizal status (i.e., arbuscular or ectomycorrhizal associations) and numerous wood traits (e.g., density; see Table S1). Variation in wood traits among species was expected to translate to a pronounced range in decomposition rates (Lee et al. 2022).

To prepare the FWM pieces, we first sourced ~ 20 individuals of each tree species from only the YMF location to minimize potential within-species variation in wood traits associated with environmental and/or genotypic variation. Our study was not designed to test how the traits of woody species affect decomposition. Rather, we chose species that represented realistic trait variation to investigate the generality of our findings about CWM effects across wood traits. To further minimize within-species trait variation we also used only wood cut from the main bole (i.e., trunk) of the trees we harvested. We selected naturally regenerating saplings of each of the five species. Saplings with a diameter of between 6 and 8 cm at 1.37 m above ground-level were selected, felled, stripped of branches and then transported to Yale's main campus (New Haven, CT, USA) to be cut into 10-cm long FWM pieces within 5 days of harvest. Our choice to use smaller diameter trees meant heartwood formation was essentially absent and so did not create within- and among-FWM variation in decomposition rates (Noll et al. 2016).

We generated variation in deadwood volume by selecting FWM pieces from the boles that spanned a diameter range of 3.5 cm to 8.0 cm, generating fivefold variation in FWM volume. Deadwood volume strongly influences decomposition rates given that smaller deadwood surface area to volume ratios (i.e., wider diameters) impede rates of colonization by microbial and animal decomposers (Oberle et al. 2018). We measured the diameter of the ends of each cut FWM piece to the nearest 0.1 cm with calipers to determine volume of each piece. As with traits, we varied deadwood volume to look at the generality of CWM effects on wood decomposition and not to investigate volume effects per se. We distributed FWM pieces based on their initial volume equally among locations and, within a location, matched FWM volumes in the microsites that were grouped spatially into a pair, one away from and one next to CWM. We used smaller rather than large diameter classes of downed deadwood because they are especially relevant to understanding field decomposition rates in managed forest because most woody debris inputs to the forest floor are often in the smaller size classes (< 15 cm dia.) (Kruys et al. 1999; Pedlar et al. 2002). In eastern U.S. forests, small diameter classes (~ 10 cm or less) dominate downed woody material stocks (Woodall et al. 2013).

FWM pieces were cut on a bandsaw with bark left on, and then uniquely numbered with an aluminum tag affixed with a short screw. Tagged FWM pieces were placed in an oven for ~ 2 h at 72 °C, following U.S. National Firewood Task Force recommendations for heat treating FWM pieces to prevent movement of pests and pathogens among forests. The aim of this treatment is to maintain internal wood temperatures of 71.1 °C for a minimum of 75 min. The treatment does not influence the chemistry nor alter the moisture content of the wood because of its short duration. Although we deliberately chose our harvest location to minimize pest risk (e.g., both emerald ash borer and Asian longhorn beetle—the two dominant hardwood insect pests in the region—were both undetected at our location at the time of tree harvest in April 2016), we heat-treated the FWM pieces as a precaution given that we were distributing them across the east coast. Once heat treated, the initial fresh mass (to 0.01 g) of the FWM pieces was measured at the same time as the end diameters were recorded. FWM pieces were then stored in paper bags before being placed in the field in May 2016.

When preparing the FWM pieces, between 7 and 25 pieces per species (with the exact number determined by those in excess of the number needed for field placement) were returned to the ovens and dried to constant mass at 70 °C, to estimate the initial moisture of the FWM pieces for field placement. Six of these FWM pieces per species were then used to determine total C and N concentrations. These data were used–along with the dimensions data–to estimate the initial wood density, mass and C and N contents for each species (Table S1). We used the initial moisture data, along with the fresh mass and dimensions data for every FWM piece placed in the field, to estimate the initial density of each piece.

FWM decomposition

On retrieval of the FWM pieces, any adhering soil, leaves and fungal cords were brushed away before the pieces were placed into individual Ziploc bags and returned to the lab where they were stored at 5 °C until further processing. In the lab, the FWM pieces were gently brushed clean of any remaining external material, before fresh mass was recorded along with the piece's length and end diameters (to estimate final volume for use in final density calculations), as well

as visual scores of termite activity and decomposition stage. Next, one third of the transect FWM pieces (10 per species per location) were selected from five paired microsites arrayed at the start, end and along the transects. These FWM pieces were drilled with an 8-mm dia. bit across the length of each piece to generate sawdust for additional measurements. All FWM pieces were then weighed and placed in an oven at 70 °C and dried to constant mass before being weighed again to determine wood dry mass and moisture content.

Using the sawdust samples, we measured total C concentrations and an estimate of active microbial biomass in the decomposing wood. The sawdust was separated into two samples, with one set of samples dried to 70 °C, then ball milled to a fine powder before analysis for total C (and N concentrations for initial FWM pieces) using an elemental analyzer (Costech ESC 4010, Costech Analytical Technologies Inc.,Valencia, CA). We used these total C measurements to calculate mass C loss given the high prevalence of termites at our most southerly location (King et al. 2013). Specifically, we were concerned that termite colonization of the decomposing FWM pieces could obscure density and mass loss estimates because termites bring mineral soil into decomposing wood. Determining percentage mass C loss corrects for mineral-soil contamination (Ulyshen and Wagner 2013).

The second sawdust sample, which was kept fresh at 5 °C until analysis, was used to estimate active microbial biomass following Maynard et al. (2018). Briefly, we used a modified substrate-induced respiration approach (Beare et al. 1990; Fierer et al. 2003) that incubates at 20 °C a fresh sawdust subsample with autolyzed yeast-extract in DI water as a labile C substrate and measures respiration over a 4-h period with an infrared gas analyzer (IRGA; Model LI-7000, Li-Cor Biosciences, Lincoln, Nebraska, USA). Carbon dioxide concentrations were converted to rate of C–CO_2 production, as mass C produced per hour per dry mass-equivalent wood. The short timescale of the assay has been shown to be a good proxy for total microbial biomass in soils and litters (Fierer et al. 2003; Frey et al. 2004) and is highly correlated with direct measures of fungal biomass (Beare et al. 1990). However, we refer to the assay as a measure of total microbial activity since it does not separate fungal and bacterial activity in deadwood. The same set of additional assays was performed for one maple and one pine FWM piece from every microsite in the common gardens at YMF for both the 25- and 49-month harvests.

Microclimate and soil measures

We measured the end diameters, length and decomposition stage of the CWM adjacent to where we placed the FWM pieces and of all CWM in the common gardens. For all microsites we took spot measurements of soil temperature and moisture to 5-cm depth. Per microsite, three spot soil measurements were taken and averaged for temperature using a stainless-steel thermometer and for volumetric soil moisture with a time domain reflectometry probe (Campbell Hydrosense™), inserted at a ~ 45° angle with 12-cm rods. Microclimate measurements were taken at six additional time points and for different seasons over the 25-month field-incubation period. The repeated discrete point measurements were intended to capture relative differences in soil microclimate variables over space, which are considered robust across time (Vachaud et al. 1985; Vanderlinden et al. 2012).

At establishment of the observational transects, we sampled surface (0–5 cm depth) soils at each of the 30 microsites at each location by taking ~ 10 2-cm dia. cores and pooling them into a Ziploc bag, which yielded 150 soil samples total. Soil sampling for the common gardens was carried out the same way, with the exception that soils were pooled per garden and collected in June 2018 when the FWM pieces were harvested. All soils were characterized for pH, active microbial biomass, soil organic matter (SOM), total C and N concentrations, C mineralization rates, and net potential N mineralization and nitrification. Prior to analysis, we homogenized and then passed the soils through a 4-mm sieve. We did not use a 2-mm sieve because, to pass effectively through that sieve size, we would have had to air dry the soils and, along with re-wetting, this would have altered the microbial process rates that we then measured.

For pH, we mixed each sample with water in a 1-to-1 volumetric ratio and measured the pH of the supernatant after 10 min using a benchtop meter (VWR sympHony Sb70p; Allen 1989). For active microbial biomass (Wardle and Ghani 1995) we used a modified substrate-induced respiration method, similar to that used for the wood samples, that measures

rates of CO_2 efflux over a 4-h incubation period (West and Sparling 1986). Soil total C and N was estimated on ball-milled samples as described for the wood samples, and the ball-milled samples were also used to determine SOM concentrations via loss-on-ignition, where we estimated SOM by calculating mass loss of soils heated at 375 °C for 18-h in a muffle furnace.

We estimated microbially-available C concentrations using an assay that determines potential CO_2 production rates over a 28-d incubation period at 20 °C (Bradford et al. 2008). The resulting estimate of labile C is calculated as the cumulative CO_2 efflux over the course of the incubation period through integration of five CO_2 efflux measurement points (days 1, 4, 11, 21 and 28). Soils were maintained at 65% water-holding capacity (WHC) over the incubation and were incubated between measurements at 20 °C under a humid atmosphere. Soil WHC was checked weekly to maintain 65% WHC, which is within the optimal range for microbial activity (Paul et al. 2001; Langenheder and Prosser 2008). Finally, to determine potential rates of net N mineralization and net nitrification, we used a 28-d N mineralization assay (Robertson et al. 1999), with soils incubated as for the C-mineralization assays. Initial and 28-day extractions were analyzed for NH_4^+ and NO_3^- concentrations using a flow analyzer (Astoria 2, Astoria-Pacific, Clackamas, Oregon, USA). Net potential nitrification is the difference in $[NO_3^-]$ between the incubated and initial samples, and net potential N mineralization is the difference between the initial and final sum of $[NH_4^+]$ and $[NO_3^-]$ over the 28-d incubation period.

Inferential analyses

We constructed a structural causal model (SCM, Fig. 1) that depicted the causal pathways of CWM, climate and wood trait effects on decomposition rates. We used the SCM to guide our statistical modeling to robustly estimate the effect size of CWM proximity on decomposition rates. We also used the SCM to evaluate which causal pathways, mediated through the presence of CWM, most likely operated to influence wood decomposition rates by including and excluding causal predictors of wood decomposition, such as soil moisture, and assessing the influence on the size of the regression coefficient for CWM proximity. Our decision regarding which variables to include in the SCM, and hence the statistical models, was based on known biological mechanisms that relate each predictor to the response variable rather than model selection (Hobbs et al. 2012).

For our statistical modeling we used hierarchical mixed models. The structure of these linear mixed models (LMMs) allowed us to represent the spatial structure of our observational transects and common gardens with FWM pieces clustered per microsite, and microsites clustered per location. We used the lme4 package (Bates et al. 2015) in the statistical program R (version 4.2.0; R Core Development Team 2023). For the random effects, microsite was nested within location. Fixed effects included proximity to CWM as a binary variable (i.e., 1 for proximate, 0 for distant), FWM traits (i.e., initial wood density or N content), FWM volume, and microclimate (i.e., soil temperature and moisture). To estimate FWM decomposition rates, we used percentage mass, density and C loss as response variables. Given the distribution of the decomposition response variables, we fit models using the lmer function for Gaussian-distributed data.

There is potential for strong correlations among our climate predictors and so we evaluated the square-root of the variance inflation factors (VIFs) for the predictors in a model including only main effects. If values were < 2.0 we initially retained the predictors in the same model, given the expectation that collinearity was low enough to limit its influence on the coefficient estimates of the predictors. We next constructed models with the retained predictors that included ecologically relevant, two-way interactions, such as initial wood density by soil temperature. To evaluate the robustness of the coefficient estimates from these models, we conducted a sensitivity analysis following Bradford et al. (2019) to evaluate how inclusion/exclusion of interactions, and different forms of the same predictor (e.g., mean vs. low soil temperature) or response (e.g., density vs. mass C loss), influenced our conclusions. Following this sensitivity analysis, we calculated r^2 values for the reported models following Nakagawa and Schielzeth (2013) to retain the random effects structure.

To examine the mean effect size of proximity to CWM on decomposition, we took two approaches. We first compared the size of the standardized coefficients, where standardizing involved centering continuous and binary variables by subtracting the

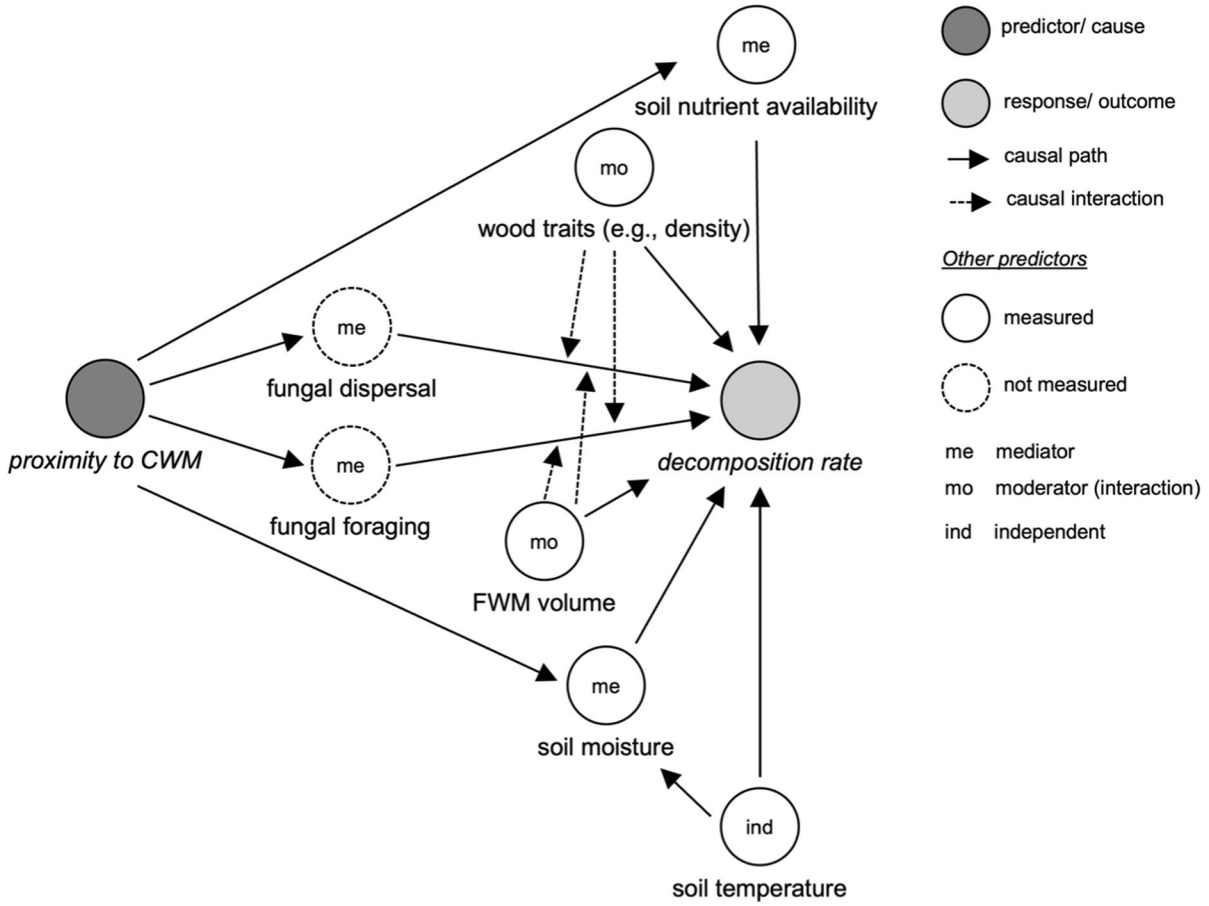

Fig. 1 Structural causal model (SCM) of CWM proximity effects on decomposition rates of the FWM pieces. We use the causal assumptions depicted in the SCM to ensure that we are robustly estimating the causal effect size of CWM proximity and to explore the mechanisms that may mediate this causal effect. Note that the two modifiers could interact with all other predictors shown, and the other predictors (including the mediators given the potential for them to have direct effects not driven by CWM proximity) plausibly could also interact. However, for clarity those dotted arrows are not shown but are tested in the statistical modeling

mean and then dividing continuous variables by two standard deviations (Gelman 2008). This approach puts binary and continuous variables, including those with different units, on the same scale and permits unambiguous determination of the size and sign of interaction effects (Gelman 2008). Second, we plotted the influence of changing proximity, microclimate, wood traits and FWM volume on decomposition. To do this, we used the unstandardized regression relationships derived from our statistical models, held all other factors at their mean for the dataset (i.e., for all observations), and varied the predictors of interest across the range of values observed across the study.

Results

Observational transects

To estimate the conditional effect size of CWM proximity on decomposition rates, we first constructed statistical models with only CWM proximity, FWM density, FWM volume and temperature as predictors. That is, we deliberately omitted any variables that we identified as "mediators" in our SCM (Fig. 1) because inclusion of mediator variables can obscure the effect of the causal predictors that act through them (McElreath 2020). Effects of the known regional-scale controls on wood decomposition (i.e., initial wood

density, FWM volume and temperature), as well as the control under test (i.e., proximity to CWM), were clearly influential given the size of the standardized coefficients (Table 1). To evaluate these effects, we plotted these regression relationships using the unstandardized coefficients (Table 1).

Plotting the individual observations (Fig. 2a) and the regression relationships (Fig. 2b) revealed that there was considerable variation in the decomposition of the FWM pieces recovered from the observational transects, both within species and within locations. Within-species variation in decomposition of FWM pieces often exceeded among-location differences in mean decomposition rates for the species, as well as among-species variation in decomposition rates (Fig. 2). For example, at the warmest location, density loss of the individual beech FWM pieces varied from ~ 20% to more than 90% (Fig. 2a), whereas mean differences in beech decomposition were between 30 and 50% across locations and, at the same location, mean species-level differences spanned ~ 20 to 50% density loss (Fig. 1b). Even at the coldest location, where the range in decomposition was muted, density loss of the individual beech FWM pieces varied from ~ 15% to ~ 60% (Fig. 2).

Despite the high local variation in decomposition rates, plotting the regression results revealed strong mean and interactive effects of the causal variables. For example, the negative interaction between initial density and proximity to CWM (Table 1) arose because proximity to CWM accelerated the decomposition of less dense wood (i.e., pine and then maple) much more so than for denser-wood species like the oak and beech (Fig. 2b). The standardized coefficient of this interaction was approximately equivalent to the main effect of initial FWM volume, and about a third of the size of the main effect of initial wood density, which had the largest standardized coefficient (Table 1). The latter coefficient manifested as strong species-level differences in density loss, where pine FWM pieces (least dense) decomposed the slowest and oak FWM pieces (which were the densest;

Table 1 Result of linear mixed model[a] for wood density loss from the observational transect FWM pieces after 25 months of field incubation at the five eastern U.S. forest locations

Predictor Variables	Unstandardized Coefficients		Standardized Coefficients	
	Mean	SE	Mean	SE
Intercept	4.254	11.7833	**31.923**	0.6818
Proximity to CWM	**12.943**	4.3699	**2.805**	1.3553
Initial wood density (g cm^{-3})	29.248	20.0322	**14.279**	0.9144
Initial wood volume (cm^3)	− 0.004	0.0327	**− 4.923**	1.0911
Soil temperature (℃)	− 0.699	0.5412	**9.958**	1.3633
Proximity × density	**− 18.286**	7.4939	**− 4.438**	1.8188
Density × volume	− 0.058	0.0556	− 1.893	1.8179
Density × temperature	**3.471**	0.9311	**6.847**	1.8370
Fixed r^2	30.1	na	30.1	na
Full r^2	44.9	na	44.9	na

Coefficients (mean ± SE), significance and r^2 values are reported and are used to evaluate the influence of proximity to coarse woody material (CWM), initial wood characteristics (density and volume), and microclimate (mean soil temperature across the field-incubation period) on wood density loss. Unstandardized coefficients are used to plot regression relationships (see Fig. 2b), and standardized coefficients are reported to facilitate comparisons of the effect size of predictor variables on different unit scales; and to facilitate interpretation of main effects involved in the two-way interactions. Significant ($P < 0.05$) coefficients are shown in bold font

[a]Mean coefficients and standard error (SE) estimated using an MCMC sampling approach, significance with the Satterthwaite approximation for REML models, and model r^2 values using a method that retains the random effects structure. Random effects assumed a common slope and for the intercept Microsite (1 to 150) was nested within Location (5 total, with 30 microsites each). Five FWM pieces (one of each species) were placed in each microsite, meaning 750 FWM pieces total were deployed. The model used 745 observations given that five FWM pieces were not recovered. In the first column, continuous predictor variables are shown in regular font and binary predictors in italics. The model was fit with a Gaussian error distribution. Model r^2 values are given for the fixed and full (i.e., fixed + random) effects. The largest square-root of the variance inflation factor (VIF) value was 1.002 for the main predictor variables when run in a model without interactions and with unstandardized predictors, indicating correlation among the predictors shown was low enough (i.e., VIF < 2.0) to be included in the same model. na = not applicable

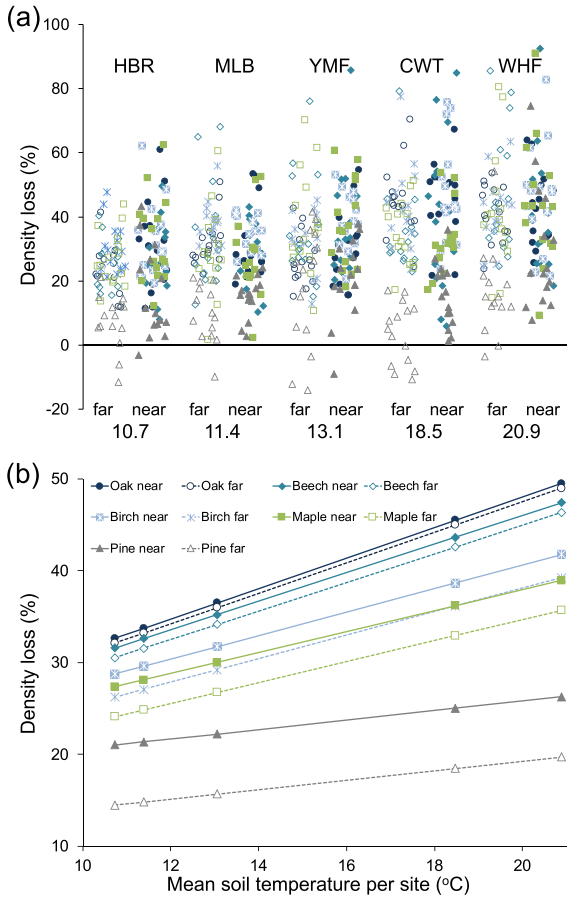

Fig. 2 Wood decomposition of FWM pieces of five tree species were strongly affected by main and interaction effects of microclimate, wood traits and proximity to downed coarse woody material (CWM) across observational transects. Decomposition is represented as wood density loss, as percentage of original density, after 25 months of field incubation at five locations spanning a climate gradient in eastern U.S. temperate, mixed forest. FWM pieces were 10-cm long and placed far from (open symbols: far) or next to (closed symbols: near) existing CWM in the forest understories. Plate **a** shows the individual data points and plate **b** plots the mean effects of the predictors and their interactions as estimated from the regression models. That is, in (**a**) are observations from 745 FWM pieces, with the FWM pieces far from CWM on the left and next to CWM on the right grouped under each location name (e.g., HBR) and mean soil temperature (e.g., 10.7 °C). Observations are jiggered within each grouping so that they can be discerned. At each location, 150 FWM pieces were placed in groups of five (1 per species) in 15 paired microsites either far or next to CWM, meaning that each location had 30 FWM pieces per species, giving 750 FWM pieces total across the locations, of which 5 were not recovered. Symbol shapes depict tree species, with the four deciduous broad-leaf species shown in blue and green, and the evergreen, needle species shown in grey. The same symbol design is used in (**b**) which plots the linear model coefficients (Table 1), with symbols only shown in this plot to identify species and to identify the mean soil temperature of each location. Plotting the model using the conditional coefficients reveals how the effect of proximity to CWM is strongly dependent on the species identity of the FWM pieces, with oak decomposition very little influenced by proximity, whereas pine decomposition responded strongly. To estimate mean density loss, we used the predictor mean values for soil temperature and initial density for each species, along with proximity to CWM as a binary variable (0 = far, 1 = near), with all other predictors held at their mean values

Table S1) the fastest (compare the intercepts of the slopes in Fig. 2b). The interaction between initial density and mean soil temperature (Table 1) revealed that relative—as well as absolute–species-level differences were greater at the warmer locations (Fig. 2b). The relative and absolute magnitude of the main and interactive effects of the controls we investigated were similar when we expressed decomposition as either percentage mass or C loss (compare Tables S2 and S3). As such, potential translocation of mineral soil into decomposing FWM pieces by termites did not appear to influence modeled effects of trait, climate and proximity to CWM on decomposition. We therefore continue to focus our main results on density loss.

We next ran models where we included the mediator variables that we measured (Fig. 1) to evaluate if they influenced the coefficient estimate for CWM proximity, which would then suggest that the CWM proximity effect was, at least in part, mediated by the influence of CWM on these predictors. The measures related to soil nutrient cycling, such as potential net N mineralization rates, were minor or inconsistent predictors of decomposition rate and had no influence on the coefficient estimate for CWM proximity. Equally, inclusion of soil moisture as a predictor did not affect the influence of CWM proximity but it did for temperature. Specifically, soil moisture and temperature were moderately correlated (Pearson's $r = -0.542$, df = 148) and strongly influenced one another's coefficient estimates. The correlation arose because the warmer locations had drier soils on average. Given that moisture and temperature are considered strong controls on wood decomposition rates (Moore et al. 1999), we ran models with either microsite soil temperature or moisture to evaluate if inclusion of either influenced the proximity to CWM main and interaction effects. They did not (Tables 1 and S4) and in

subsequent analyses we used soil temperature as our climate predictor because that model explained more variation and because we found that FWM pieces within the same microsite could differ markedly in wood moisture content, suggesting a disconnect between soil moisture and the moisture content of surface-placed, downed wood.

Given the fact that soil moisture in a microsite responded minimally to CWM proximity and was a poor surrogate for observed moisture content of the FWM pieces, we considered running FWM moisture content (at harvest) as a predictor. We did not pursue this analysis because wood moisture is both a predictor and outcome of decomposition (Dix 1985). Consequently, the causal direction(s) of the correlation (Pearson's $r = 0.435$) between wood moisture and density loss is uncertain. Equally, we did not run active microbial biomass as a predictor–which was correlated with mass C loss (Pearson's $r = 0.438$)—because we could not discern the causal role of microbial biomass from the associated controls on decomposition such as CWM proximity and temperature. Yet the positive correlations between decomposition and wood moisture content, as well as active microbial biomass, are consistent with expected changes in wood biophysical variables as it is decomposed by wood-rot fungi (Dix 1985; Bradford et al. 2021). Further, the coefficients for the controls we evaluated were robust to statistical model structure (e.g., inclusion of two-way interactions, Table S4), the form of the predictor (e.g., low vs. mean soil temperature; initial wood density vs. initial wood N content, Table S4), as well as the form of the response variable (i.e., density, mass or C loss; compare Tables 1, S2, S3). As such, regardless of the analytical decisions that we made, our observational transect data were consistent in identifying proximity to CWM as a control that accelerates wood decomposition, and in finding that the effect did not appear mediated via CWM influences on soil moisture or nutrient availability.

Common gardens and time course data

The common gardens gave us greater experimental control to attribute effects to CWM presence because they reduced the likelihood that unmeasured variables, which might be associated with accumulation of CWM, could instead explain the effects of CWM proximity in the observational transects. Again, following our SCM, we began analysis of the common garden data by evaluating the effects of predictors that were not mediating variables of either CWM proximity or temperature. As with the transect data, maple decomposed faster than pine FWM pieces and pieces with larger initial volume decomposed more slowly (Fig. 3b). The standardized coefficient for initial density was ~ 4-times larger than any of the other predictors, likely reflecting the strong contrast in traits between the maple and pine FWM, which included the maple pieces having denser wood, higher %N content and presumably lower secondary chemical concentrations (Tables S1 and S5). The standardized coefficient for the main effect of proximity to CWM was essentially the same size as those for initial FWM volume and mean soil temperature, suggesting again that proximity effects can be as large as known predictors in a regional-scale analysis (Table S5).

Proximity accelerated the decomposition rate of the FWM pieces and its absolute influence on decomposition was magnified as mean soil temperature across locations increased (Fig. 3b, Table S5). The positive temperature relationship was dampened for FWM pieces of larger volume (Fig. 3b), altering the manifestation of the CWM proximity by temperature interaction. The dampening effect was so pronounced that the estimated mean effect of soil temperature on the FWM pieces with the widest diameters and hence largest volumes was slightly negative for FWM pieces away from CWM, whereas those FWM pieces proximal to CWM maintained a positive temperature-decomposition relationship (Fig. 3b). As with the transect data, we analyzed proximity to CWM as a binary variable but the interpretation of the statistical models is essentially unchanged if CWM volume is used.

Despite the strong mean effects of the CWM proximity, trait and temperature predictors, FWM pieces in the common gardens at each location varied extensively in the amount to which they were decomposed after 25 months (Fig. 3a), mirroring the variation seen in the observational transects. Nevertheless, the controlled experimental nature of the common gardens likely accounts for why the fixed effects explain more variation (43.9%) than with the transect data (30.1%), despite having only approximately one-third of the observation numbers ($n = 238$ FWM pieces recovered of 240 placed in the field versus 745 FWM pieces recovered of 750 placed in the field for the transects).

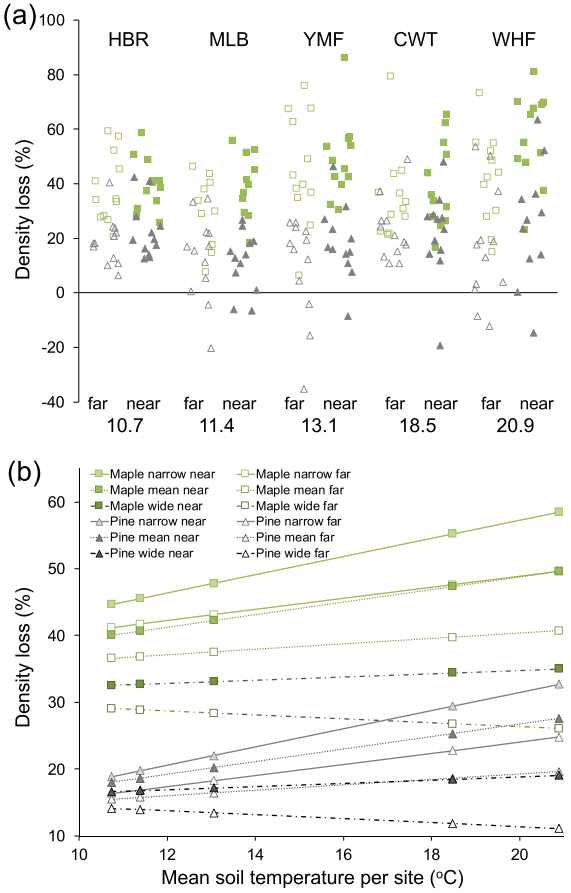

Fig. 3 Wood decomposition of FWM pieces of both sampled tree species was strongly affected by main and interaction effects of microclimate, wood traits and presence of downed coarse woody material (CWM) in experimental common gardens. Decomposition is represented as wood density loss, as percentage of original density, after 25 months of field incubation at five locations spanning a climate gradient in eastern U.S. temperate, mixed forest. FWM pieces were 10-cm long and in common gardens with zero (open symbols) or high-density (closed symbols) CWM abundance in the forest understories. Plate **a** shows the individual data points and plate **b** plots the mean effects of the predictors and their interactions as estimated from the regression models. That is, in (**a**) are observations from 238 maple and pine FWM pieces, with the FWM pieces in zero-CWM gardens on the left ('far') and high-CWM gardens on the right ('near') above each location name and mean soil temperature. Observations are jiggered within each grouping so that they can be discerned. At each location, 48 FWM pieces were placed in groups of two (1 per species) in 24 paired microsites, with 12 microsites in no-CWM gardens and 12 in high-CWM gardens, meaning that each location had 24 FWM pieces per species, giving 240 FWM pieces total across the locations, of which 2 were not recovered. The same symbol design is used in (**b**) which plots the linear model coefficients (Table S5), with symbols only shown in this plot to identify species and the mean soil temperature of each location. Plotting the model using the conditional coefficients reveals how decomposition is co-dependent on proximity to CWM, species identity, mean temperature of the location and FWM volume, where the greatest decomposition was observed with narrow maple FWM pieces, at the warmest location, which were next to CWM. To estimate mean density loss, we used the predictor mean values for soil temperature and initial density for each species, along with proximity to CWM as a binary variable (0 = far, 1 = near), and FWM volumes reflecting the observed range for these experimental FWM pieces (where narrow = 119 cm^3, mean = 229 cm^3 and wide = 410 cm), with all other predictors held at their mean values

As with the transects, we evaluated whether the CWM proximity effects were mediated by modification of the microclimate or soil nutrient availabilities (Fig. 1). The soil nutrient variables neither obscured the CWM proximity effect nor had meaningful effect sizes on decomposition. Also, as seen with the transect data, soil moisture did alter the soil temperature effect given the correlation between the two predictors (Pearson's $r = -0.594$, df = 118) but did not influence the CWM proximity effect.

Given that the influence of controls on wood decomposition can change with time of field incubation (Oberle et al. 2020), we placed additional maple and pine FWM pieces in the common gardens at the YMF location and harvested them at 13 and 49 months, as well as 25 months. The influence of harvest time was of similar magnitude to initial wood density, and it interacted positively with initial density, wood volume and CWM proximity (Table S6). These interactions meant that the influence of initial density and CWM proximity strengthened across time but that initial volume differences among the FWM pieces became less consequential for decomposition (Fig. 4). Notably, as for the observational transect data, the influence of proximity to CWM was greater when decomposition was instead expressed as percentage mass C loss, and for that model the fixed effects explained more variation (~79%) than they did for density loss. As such, positive effects of proximity to CWM were consistently observed regardless of the statistical analysis decisions we made about which predictors and response variables to model (Table S6). By contrast, our findings were dependent on study design decisions, whereby this temporal analysis revealed that CWM proximity effects likely strengthen over time (as revealed by diverging near versus far lines in Fig. 4b).

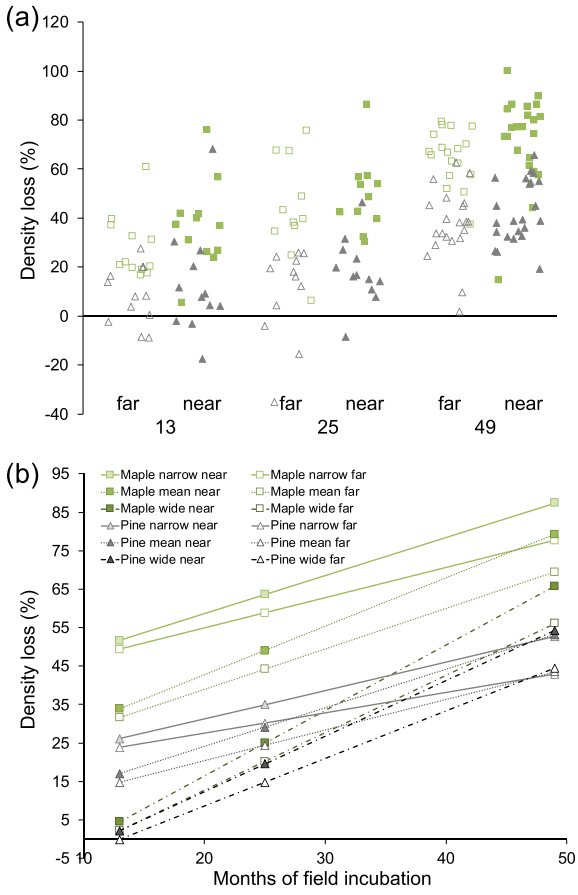

Fig. 4 Wood decomposition of FWM pieces of two tree species were strongly affected by main and interaction effects of time, wood traits and presence of downed coarse woody material (CWM) in experimental common gardens. Decomposition is represented as wood density loss after 13, 25 and 49 months of field incubation at one location in northeastern U.S. temperate, mixed forest. FWM pieces were 10-cm long and in common gardens with no- (open symbols) or high- (closed symbols) CWM abundance in the forest understory. Plate **a** shows the individual data points and plate **b** plots the mean effects of the predictors and their interactions as estimated from the regression models. That is, in (**a**) are observations from 181 FWM pieces, with the FWM pieces in no-CWM gardens on the left ('far') and high-CWM gardens on the right ('near') above each collection point. Observations are jiggered within each grouping so that they can be discerned. When establishing the common gardens, 192 FWM pieces were placed in groups of eight (4 per species) in 24 paired microsites, with 12 microsites in no-CWM gardens and 12 in high-CWM gardens, meaning that each garden type had 48 FWM pieces per species. One FWM piece of each species was collected from each microsite at 13 and 25 months, and two per species at the 49-month collection, albeit 11 FWM pieces placed in the field could not be found. The same symbol design is used in (**b**) which plots the linear model coefficients (Table S6), with symbols only shown in this plot to identify species and the months of field incubation. Plotting the model using the conditional coefficients reveals how the effect of proximity to CWM strengthens as field incubation time increases, regardless of species identity or FWM volume (i.e., width). To estimate mean density loss and FWM volumes see legend to Fig. 3

Discussion

Given the importance of CWM as a resource from which wood-rot fungi can colonize new deadwood inputs, we hypothesized that FWM pieces adjacent as opposed to away from CWM would decompose faster. Our data are consistent with CWM proximity as a causal predictor that accelerates the decomposition of new deadwood inputs to forest floors (Figs. 2, 3 and 4). The size of this proximity effect was dependent on the species identity of the deadwood inputs, where the decomposition of species with higher initial wood density and N content, such as red oak, responded little to CWM proximity whereas those species with the lowest density wood, namely red maple and eastern white pine, responded strongly (Fig. 2). Our inferences about these main and interactive effects of CWM proximity were robust to the analytical decisions we made regarding how to represent decomposition (e.g., mass C vs. density loss) and which predictors to include in our models (Tables S2-4). The fact that such decisions also consistently identified well-established regional controls such as climate and wood traits (Oberle et al. 2020; Seibold et al. 2021), within the milieu of high and unexplained local and regional variation in the decomposition rates of downed deadwood, should build confidence that CWM proximity will be reproducible as a regional-scale control, at least within eastern U.S. temperate forests.

Fine-scale estimates of CWM density across the U.S. are available through the Forest Inventory and Analysis database (Woodall et al. 2013; Wilson et al. 2013), and CWM stocks vary predictably with forest growth and management (Zhu et al. 2017; Pugh et al. 2019; Woodall et al. 2021). Further, the density of CWM across a forest stand is relatively straightforward to measure (Waddell 2002). These databases and measurements, as well as those available in many other countries (Russell et al. 2015), could be leveraged to integrate and parameterize CWM proximity as a control within C cycle and ecosystem models that estimate wood decomposition. However, integration of our findings into models would likely benefit from an understanding of how increasing distance from CWM translates to decomposition rates, whereas we simply investigated proximity as a binary variable. Further, representation of new ecological variables in C cycle models requires that they meaningfully

change model predictions and confidence (Kyker-Snowman et al. 2022). For wood decomposition, confidence in model projections is currently low (Keenan et al. 2013), suggesting ample need to resolve parameter and structural uncertainties. Our work helps to address these uncertainties, by identifying and quantifying a heretofore underappreciated control that influences regional-scale wood decomposition dynamics.

We reasoned that we could not directly test, in the field and without introducing numerous experimental artifacts, the hypothesized causal mechanism that CWM proximity effects were mediated through higher fungal colonization rates. Instead, we evaluated alternate mediating mechanisms that might explain the positive effects of CWM proximity (Fig. 1). By measuring soil moisture in each microsite, we tested the possibility that CWM creates favorable microclimate conditions that facilitate higher wood-rot fungal activity (Rayner and Boddy 1988). The low collinearity between soil moisture and CWM proximity in the regression models, and the fact that inclusion of moisture did not affect the CWM proximity coefficient, suggested the mechanism of CWM effect was likely not mediated via modification of the microclimate. Equally, none of the soil variables related to C and N availability emerged as a reliable predictor of field decomposition rates, and nor did their inclusion in models obscure the CWM proximity effects. As such, there was little evidence that CWM created a more fertile microenvironment that in turn permitted more rapid wood decomposition via translocation of nutrients via fungal hyphae into the decomposing FWM pieces (Cairney 2005). Lastly, there was no evidence for unmeasured variables that might have created a spurious association between CWM proximity and decomposition rates in the observational transects, because the CWM proximity effects were positive and of similar magnitude in the common gardens. As such, our work suggests that CWM proximity is a causal driver of faster wood decomposition rates. The precise mechanism(s) mediating this effect remain unresolved. However, the substantial literature on fungal community dynamics as drivers of marked differences in wood decomposition rates in boreal and temperate forests (Toljander et al. 2006; van der Wal et al. 2015; Lustenhouwer et al. 2020; Smith and Peay 2021), builds evidence for the likelihood that CWM proximity effects are mediated via more rapid fungal colonization of new inputs of downed dead wood.

Regardless of the causal mechanism(s) underpinning the CWM proximity effects, we observed within-location variation in wood decomposition rates of the same tree species which was larger than the magnitude of among-location variation in mean decomposition rates. Marked within-location variation in wood decomposition rates is to be expected (Boddy et al. 1989; Bradford et al. 2014, 2021), and our regression models consequently had relatively low explanatory power (e.g., 30% for the observational transects, Table 1) when compared to numerous other multi-location studies (Moore et al. 1999; Pietsch et al. 2014; Zhu et al. 2017). The difference in explanatory power most likely arises because our study had high within-location replication across local gradients in controls, whereas many prior studies focus instead on minimizing within-location variability and maximizing the number of locations (Bradford et al. 2016). To explore the potential implications of these differences in study design for understanding controls on wood decomposition, we conducted a post-hoc analysis by aggregating our observational transect data at three different spatial grains: (a) mean values per climate (at the level of location) or by species, (b) mean values per location per species, and (c) individual FWM pieces (i.e., not aggregated). We then ran univariate regressions with climate or initial wood density as predictors.

When microclimate was aggregated to a location-level mean, or initial wood density to a species-mean, ~ 90% and 65% of the variation in these data were explained, respectively (Fig. 5a, d). When aggregated at a finer resolution to represent mean values per species at each location (Fig. 5b, e), variation explained dropped to 17% for microclimate and ~ 42% for traits, and even further (8% and 17%, respectively) for the individual data (Fig. 5c, f). The analysis shows that aggregating data on climate and trait controls at increasingly coarse spatial grains – akin to a focus on only among-location predictors – can flip conclusions based on variance explained about the relative influence of different controls (Hu et al. 2018; Joly et al. 2023). The analysis equally highlights that care must be taken to match the scale of inference (e.g., means vs. individual observations) about controls to the grain at which they influence the response variable (Ruel and Ayres 1999; Gelman et al. 2007; Bradford et al. 2014). Consequently, by focusing our inference on individual observations we identified CWM

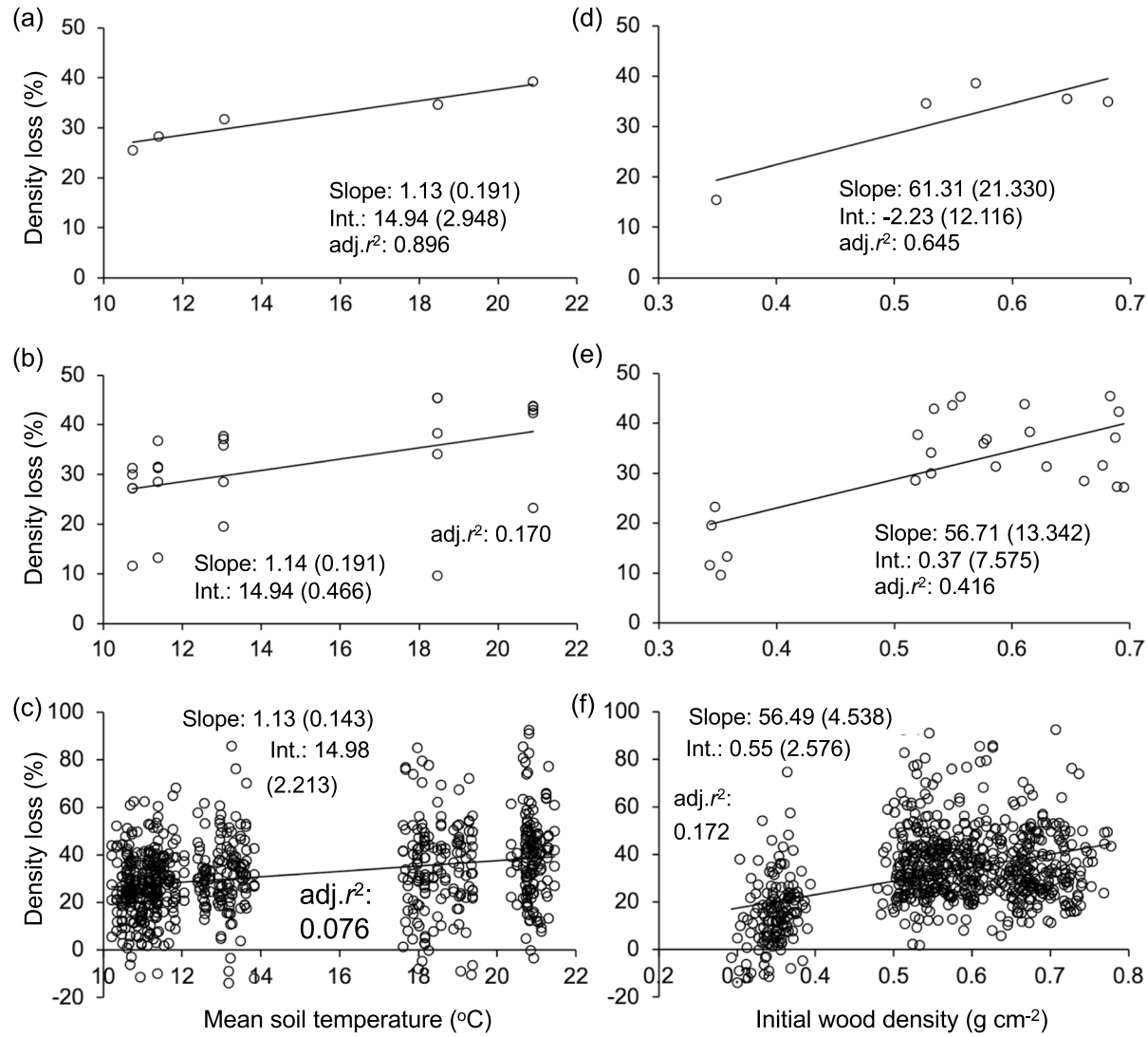

Fig. 5 Univariate regressions of wood decomposition of five tree species in relation to soil microclimate (**a**–**c**) and initial wood density (**d**–**f**). The amount of variance explained (adjusted r^2) in these data (from the observational transects: Fig. 1a) decreases markedly as the predictor and response variables for the 745 FWM pieces are increasingly disaggregated from the location (**a**) or species (**d**) level means where n = 5, to representation as species by microclimate means (**b** and **e**, n = 15), to the 745 individual observations themselves (**c** and **f**). See Fig. 1 legend for details on the study design. Note that the regression coefficients (with standard error in parentheses) for the predictors are for the univariate relationships, making them non-conditional, and so they differ to those presented in the linear mixed model shown in Table 1 and plotted in Fig. 1

proximity as a causal predictor exerting and interacting with known climate and trait controls on wood decomposition at a regional scale.

Our study adds to growing evidence that multiple controls operate collectively and conditionally on wood decomposition rates at regional scales (Oberle et al. 2018, 2020; Hu et al. 2018; Bradford et al. 2021). For example, the effects of initial wood density and proximity to CWM strengthened over time, whereas the influence of FWM volume decreased. This temporal conditionality in effect sizes, in addition to our identification of CWM proximity as a control on wood decomposition, emphasizes that future work should be conducted at multiple temporal and spatial grains (Harmon et al. 2020), and move beyond asking which control is dominant

(because the answer will be context dependent). Our study design likely also omitted some important controls. For example, as described in the Methods we heat treated all FWM pieces prior to field placement to ensure we did not spread pests and pathogens. It is unclear as to whether this heating kills endophytic fungi, but their presence at the initial stages of wood decomposition can alter fungal colonization dynamics and decomposition rates (Cline et al. 2018). Future work is therefore needed to quantify CWM proximity effects on the decomposition of new deadwood inputs that are matched to the location where the wood was growing, removing the need for heat treatment. Such work should recognize the multicausal and scale-dependent regulation of wood decomposition rates, and how study design and analysis can dictate which controls emerge as most important (e.g., Fig. 5). Doing so will mean that future studies have a high likelihood of advancing knowledge of wood decomposition in a manner that can be used to build confidence in C cycle and forest ecosystem model projections.

If our results hold generally across eastern U.S. temperate forests, they suggest that depletion of CWM stocks in this system may have had consequent ecological effects by slowing wood decomposition rates at the ecosystem scale. Stocks of CWM in eastern U.S. forests have been depleted through overly intensive forest management, and management regimes are now being adapted in these and other forests across the world to rebuild CWM stocks (Lindenmayer et al. 2002; Pedlar et al. 2002; Woodall et al. 2021). The focus of these efforts has been the protection and restoration of forest biodiversity that relies on dead wood as refuge (e.g., in droughts or fire), as sites of seedling regeneration, and as food and habitat for many understory invertebrates and vertebrates (Stokland et al. 2012). Such efforts are likely to restore energy flows through brown food webs in forests (Currie 2003). Our results suggest that higher CWM stocks may further enhance such flows through brown food webs because higher CWM abundance will likely accelerate decomposition rates of fresh deadwood inputs. The eventual consequences of this restoration of decomposition channels in forests is not fully known but is likely to lead to improved forest health and resilience.

Acknowledgements We thank staff at Coweeta Hydrological Lab, Hubbard Brook Experimental Forest, Mountain Lake Biological Station, Yale-Myers Forest and Whitehall Forest, for facilitating the fieldwork at their research locations; the Yale Analytical and Stable Isotope Center for total C and N analyses; and the soil ecology lab at Morton Arboretum for inorganic N analyses. Thanks to the research assistants who helped with the wood and soil lab analyses: Lysa Uwizeyimana, Amma Asantewaa Agyei Boakye, Elena Karlsen-Ayala, Ben Rifkin, Adam Houston, Dana Lee, Ravikant Sharma and Annie Stoeth. Thanks also to Jonathan Schilling for guidance on designing deadwood decomposition studies.

Author contributions MAB, DSM, GFV and TWC: designed the study, which was set-up by the first three of the authors and with help from MSS, JTM and PTF at the southern sites. MAB: maintained the two northern locations and MSW, JTM, PTF, SM and CW: helped maintain the three southern locations. The experiment was harvested by MAB, DSM, GFV and CS, with assistance at various sites by PTF, JGR, NF, TWC and SK. MAB and EMB cut and prepared all the FWM pieces, and MAB worked with KRC to locate and fell saplings at YMF. EEO, AP, NF, CS and JGR: led various aspects of the lab analyses. MAB, EBW, AP, AMO, FVJ and EEO: developed the inferential analysis. MAB: collated all data, carried out the statistical analyses and wrote the original version of the paper; all authors contributed to the final version.

Funding This work was supported by U.S. National Science Foundation program grants DEB-1457614 and DEB-1926482 to MAB.

Data availability Data, metadata and code are permanently archived and openly available in the Dryad data repository. They are available as Bradford et al. (2023) with the unique DOI: https://doi.org/10.5061/dryad.0rxwdbs39.

Declarations

Conflict of interest The authors have no relevant financial nor non-financial interests to declare.

References

Allen SE (ed) (1989) Chemical analysis of ecological materials. 2nd edn. Blackwell Scientific, Oxford

Bates D, Mächler M, Bolker BM, Walker SC (2015) Fitting linear mixed-effects models using lme4. J Stat Softw 67:1–48

Beare MH, Neely CL, Coleman DC, Hargrove WL (1990) A substrate-induced respiration (SIR) method for measurement of fungal and bacterial biomass on plant residues. Soil Biol Biochem 22:585–594. https://doi.org/10.1016/0038-0717(90)90002-H

Boddy L (2000) Interspecific combative interactions between wood-decaying basidiomycetes. FEMS Microbiol Ecol 31:185–194. https://doi.org/10.1111/j.1574-6941.2000.tb00683.x

Boddy L, Swift MJ (1984) Wood decomposition in an abandoned beech and oak coppiced woodland in SE England.: III. Decomposition and turnover of twigs and branches. Ecography 7:229–238. https://doi.org/10.1111/j.1600-0587.1984.tb01125.x

Boddy L, Owens EM, Chapela IH (1989) Small scale variation in decay rate within logs one year after felling: Effect of fungal community structure and moisture content. FEMS Microbiol Lett 62:173–183. https://doi.org/10.1111/j.1574-6968.1989.tb03691.x

Boddy L, Frankland JC, van West P (2008) Ecology of saprotrophic basidiomycetes. Academic Press, London

Bradford MA, Davies CA, Frey SD et al (2008) Thermal adaptation of soil microbial respiration to elevated temperature. Ecol Lett 11:1316–1327. https://doi.org/10.1111/j.1461-0248.2008.01251.x

Bradford MA, Warren RJ II, Baldrian P et al (2014) Climate fails to predict wood decomposition at regional scales. Nature Clim Change 4:625–630. https://doi.org/10.1038/nclimate2251

Bradford MA, Berg B, Maynard DS et al (2016) Understanding the dominant controls on litter decomposition. J Ecol 104:229–238. https://doi.org/10.1111/1365-2745.12507

Bradford MA, McCulley RL, Crowther TW et al (2019) Cross-biome patterns in soil microbial respiration predictable from evolutionary theory on thermal adaptation. Nat Ecol Evol 3:223–231. https://doi.org/10.1038/s41559-018-0771-4

Bradford MA, Maynard DS, Crowther TW et al (2021) Belowground community turnover accelerates the decomposition of standing dead wood. Ecology 102:e03484. https://doi.org/10.1002/ecy.3484

Bradford M et al (2023) Data for: Coarse woody debris accelerates the decomposition of deadwood inputs across temperate forest, Dryad, Dataset. https://doi.org/10.5061/dryad.0rxwdbs39

Cairney JWG (2005) Basidiomycete mycelia in forest soils: dimensions, dynamics and roles in nutrient distribution. Mycol Res 109:7–20. https://doi.org/10.1017/S0953756204001753

Cline LC, Schilling JS, Menke J et al (2018) Ecological and functional effects of fungal endophytes on wood decomposition. Funct Ecol 32:181–191. https://doi.org/10.1111/1365-2435.12949

Coates D, Rayner ADM (1985) Fungal population and community development in cut beech logs: III. spatial dynamics, interactions and strategies. New Phytol 101:183–198. https://doi.org/10.1111/j.1469-8137.1985.tb02825.x

Cornwell WK, Cornelissen JHC, Allison SD et al (2009) Plant traits and wood fates across the globe: rotted, burned, or consumed? Glob Change Biol 15:2431–2449. https://doi.org/10.1111/j.1365-2486.2009.01916.x

Crowther TW, Jones TH, Boddy L (2011) Species-specific effects of grazing invertebrates on mycelial emergence and growth from woody resources into soil. Fungal Ecol 4:333–341. https://doi.org/10.1016/j.funeco.2011.05.001

Crowther TW, Maynard DS, Crowther TR et al (2014) Untangling the fungal niche: the trait-based approach. Front Microbiol 5:a579. https://doi.org/10.3389/fmicb.2014.00579

Currie WS (2003) Relationships between carbon turnover and bioavailable energy fluxes in two temperate forest soils: carbon and energy in forest detritus. Glob Change Biol 9:919–929. https://doi.org/10.1046/j.1365-2486.2003.00637.x

Dickie IA, Fukami T, Wilkie JP et al (2012) Do assembly history effects attenuate from species to ecosystem properties? A field test with wood-inhabiting fungi: assembly history effects. Ecol Lett 15:133–141. https://doi.org/10.1111/j.1461-0248.2011.01722.x

Dix NJ (1985) Changes in relationship between water content and water potential after decay and its significance for fungal successions. Trans Br Mycol Soc 85:649–653. https://doi.org/10.1016/S0007-1536(85)80259-X

Edman M, Kruys N, Jonsson BG (2004) Local dispersal sources strongly affect colonization patterns of wood-decaying fungi on spruce logs. Ecol Appl 14:893–901. https://doi.org/10.1890/03-5103

EPA (2013) Inventory of US greenhouse gas emissions and sinks: 1990–2011. Environmental Protection Agency, Washington DC

Fierer N, Schimel JP, Holden PA (2003) Variations in microbial community composition through two soil depth profiles. Soil Biol Biochem 35:167–176. https://doi.org/10.1016/S0038-0717(02)00251-1

Freschet GT, Weedon JT, Aerts R et al (2012) Interspecific differences in wood decay rates: insights from a new short-term method to study long-term wood decomposition: New method to assess wood decay dynamics and rates. J Ecol 100:161–170. https://doi.org/10.1111/j.1365-2745.2011.01896.x

Frey SD, Knorr M, Parrent JL, Simpson RT (2004) Chronic nitrogen enrichment affects the structure and function of the soil microbial community in temperate hardwood and pine forests. For Ecol Manage 196:159–171. https://doi.org/10.1016/j.foreco.2004.03.018

Fukami T, Dickie IA, Paula Wilkie J et al (2010) Assembly history dictates ecosystem functioning: evidence from wood decomposer communities: carbon dynamics and fungal community assembly. Ecol Lett 13:675–684. https://doi.org/10.1111/j.1461-0248.2010.01465.x

Gelman A (2008) Scaling regression inputs by dividing by two standard deviations. Statist Med 27:2865–2873. https://doi.org/10.1002/sim.3107

Gelman A, Shor B, Bafumi J, Park D (2007) Rich state, poor state, red state, blue state: what's the matter with connecticut? Quart J Polit Sci 2:345–367. https://doi.org/10.1561/100.00006026

Hafner SD, Groffman PM, Mitchell MJ (2005) Leaching of dissolved organic carbon, dissolved organic nitrogen, and other solutes from coarse woody debris and litter in a mixed forest in New York State. Biogeochemistry 74:257–282. https://doi.org/10.1007/s10533-004-4722-6

Harmon ME, Franklin JF, Swanson FJ et al (2004) Ecology of coarse woody debris in temperate ecosystems. Advances in Ecological Research. Elsevier, Amsterdam, pp 59–234

Harmon ME, Fasth BG, Yatskov M et al (2020) Release of coarse woody detritus-related carbon: a synthesis across forest biomes. Carbon Balance Manag 15:1. https://doi.org/10.1186/s13021-019-0136-6

Harris NL, Gibbs DA, Baccini A et al (2021) Global maps of twenty-first century forest carbon fluxes. Nat Clim Chang 11:234–240. https://doi.org/10.1038/s41558-020-00976-6

Heath LS, Smith JE, Birdsey RA (2003) Carbon trends in U. S. forestlands: a context for the role of soils in forest carbon sequestration. In: Kimble JM, Heath LS, Birdsey RA, Lal R (eds) The Potential of US Forest Soils to Sequester Carbon and Mitigate the Greenhouse Effect. Lewis Publishers (CRC Press), Boca Raton, FL, pp 35–45

Hobbs NT, Andrén H, Persson J et al (2012) Native predators reduce harvest of reindeer by Sámi pastoralists. Ecol Appl 22:1640–1654. https://doi.org/10.1890/11-1309.1

Hu Z, Michaletz ST, Johnson DJ et al (2018) Traits drive global wood decomposition rates more than climate. Glob Change Biol 24:5259–5269. https://doi.org/10.1111/gcb.14357

Jackson BG, Peltzer DA, Wardle DA (2013) Are functional traits and litter decomposability coordinated across leaves, twigs and wood? A test using temperate rainforest tree species. Oikos 122:1131–1142. https://doi.org/10.1111/j.1600-0706.2012.00056.x

Jia-bing W, De-xin G, Shi-jie H et al (2005) Ecological functions of coarse woody debris in forest ecosystem. J for Res 16:247–252. https://doi.org/10.1007/BF02856826

Joly F-X, Scherer-Lorenzen M, Hättenschwiler S (2023) Resolving the intricate role of climate in litter decomposition. Nat Ecol Evol. https://doi.org/10.1038/s41559-022-01948-z

Keenan TF, Davidson EA, Munger JW, Richardson AD (2013) Rate my data: quantifying the value of ecological data for the development of models of the terrestrial carbon cycle. Ecol Appl 23:273–286. https://doi.org/10.1890/12-0747.1

King JR, Warren RJ, Bradford MA (2013) Social insects dominate Eastern US temperate hardwood forest macroinvertebrate communities in warmer regions. PLoS ONE 8:e75843. https://doi.org/10.1371/journal.pone.0075843

Kruys N, Fries C, Jonsson BG et al (1999) Wood-inhabiting cryptogams on dead Norway spruce (*Picea abies*) trees in managed Swedish boreal forests. Can J for Res 29:178–186. https://doi.org/10.1139/x98-191

Kyker-Snowman E, Lombardozzi DL, Bonan GB et al (2022) Increasing the spatial and temporal impact of ecological research: a roadmap for integrating a novel terrestrial process into an Earth system model. Glob Change Biol 28:665–684. https://doi.org/10.1111/gcb.15894

Langenheder S, Prosser JI (2008) Resource availability influences the diversity of a functional group of heterotrophic soil bacteria. Environ Microbiol 10:2245–2256. https://doi.org/10.1111/j.1462-2920.2008.01647.x

Lee M, Powell JR, Oberle B et al (2022) Initial wood trait variation overwhelms endophyte community effects for explaining decay trajectories. Funct Ecol 36:1243–1257. https://doi.org/10.1111/1365-2435.14025

Lindenmayer DB, Claridge AW, Gilmore AM et al (2002) The ecological roles of logs in Australian forests and the potential impacts of harvesting intensification on log-using biota. Pac Conserv Biol 8:121. https://doi.org/10.1071/PC020121

Lustenhouwer N, Maynard DS, Bradford MA et al (2020) A trait-based understanding of wood decomposition by fungi. Proc Natl Acad Sci USA 117:11551–11558. https://doi.org/10.1073/pnas.1909166117

Maynard DS, Covey KR, Crowther TW et al (2018) Species associations overwhelm abiotic conditions to dictate the structure and function of wood-decay fungal communities. Ecology 99:801–811. https://doi.org/10.1002/ecy.2165

McElreath R (2020) Statistical rethinking, Second. CRC Press, Boca Raton

Moore TR, Trofymow JA, Taylor B et al (1999) Litter decomposition rates in Canadian forests. Glob Change Biol 5:75–82. https://doi.org/10.1046/j.1365-2486.1998.00224.x

Nakagawa S, Schielzeth H (2013) A general and simple method for obtaining R^2 from generalized linear mixed-effects models. Methods Ecol Evol 4:133–142. https://doi.org/10.1111/j.2041-210x.2012.00261.x

Noll L, Leonhardt S, Arnstadt T et al (2016) Fungal biomass and extracellular enzyme activities in coarse woody debris of 13 tree species in the early phase of decomposition. For Ecol Manage 378:181–192. https://doi.org/10.1016/j.foreco.2016.07.035

Oberle B, Covey KR, Dunham KM et al (2018) Dissecting the effects of diameter on wood decay emphasizes the importance of cross-stem conductivity in *Fraxinus americana*. Ecosystems 21:85–97. https://doi.org/10.1007/s10021-017-0136-x

Oberle B, Lee MR, Myers JA et al (2020) Accurate forest projections require long-term wood decay experiments because plant trait effects change through time. Glob Change Biol 26:864–875. https://doi.org/10.1111/gcb.14873

Oleson KW, Lawrence DM, Bonan GB, et al (2013) Technical description of version 4.5 of the Community Land Model (CLM) (No. NCAR/TN-503+STR). https://doi.org/10.5065/D6RR1W7M

Olsson J, Jonsson BG, Hjältén J, Ericson L (2011) Addition of coarse woody debris–the early fungal succession on *Picea abies* logs in managed forests and reserves. Biol Cons 144:1100–1110. https://doi.org/10.1016/j.biocon.2010.12.029

Pan Y, Birdsey RA, Fang J et al (2011) A large and persistent carbon sink in the world's forests. Science 333:988–993. https://doi.org/10.1126/science.1201609

Paul EA, Morris SJ, Böhm S (2001) The determination of soil C pool sizes and turnover rates: biophysical fractionation and tracers. In: Lal R, Kimble JM, Follett RF, Stewart BA (eds) Assessment methods for soil carbon. CRC Press LLC, Boca Raton, pp 193–205

Pedlar JH, Pearce JL, Venier LA, McKenney DW (2002) Coarse woody debris in relation to disturbance and forest type in boreal Canada. For Ecol Manage 158:189–194. https://doi.org/10.1016/S0378-1127(00)00711-8

Pietsch KA, Ogle K, Cornelissen JHC et al (2014) Global relationship of wood and leaf litter decomposability: the role of functional traits within and across plant organs: Global relationship of wood and leaf litter decomposability. Glob Ecol Biogeogr 23:1046–1057. https://doi.org/10.1111/geb.12172

Pugh TAM, Lindeskog M, Smith B et al (2019) Role of forest regrowth in global carbon sink dynamics. Proc Natl Acad

Sci USA 116:4382–4387. https://doi.org/10.1073/pnas.1810512116

R Core Development Team (2023) R: A language and environment for statistical computing. R Foundation for Statistical Computing. Vienna, Austria. URL https://www.R-project.org/

Rayner ADM, Boddy L (1988) Fungal decomposition of wood: its biology and ecology. John Wiley & Sons Ltd., Chichester, UK

Robertson GP, Wedin D, Groffman PM et al (1999) Soil carbon and nitrogen availability. Nitrogen mineralization, nitrification, and soil respiration potentials. In: Robertson GP, Coleman DC, Bledsoe CS, Sollins P (eds) Standard soil methods for long-term ecological research. Oxford University Press, New York, pp 258–271

Ruel JJ, Ayres MP (1999) Jensen's inequality predicts effects of environmental variation. Trends Ecol Evol 14:361–366. https://doi.org/10.1016/S0169-5347(99)01664-X

Russell MB, Woodall CW, Fraver S et al (2014) Residence times and decay rates of downed woody debris biomass/carbon in Eastern US Forests. Ecosystems 17:765–777. https://doi.org/10.1007/s10021-014-9757-5

Russell MB, Fraver S, Aakala T et al (2015) Quantifying carbon stores and decomposition in dead wood: a review. For Ecol Manage 350:107–128. https://doi.org/10.1016/j.foreco.2015.04.033

Seibold S, Rammer W, Hothorn T et al (2021) The contribution of insects to global forest deadwood decomposition. Nature 597:77–81. https://doi.org/10.1038/s41586-021-03740-8

Smith GR, Peay KG (2021) Multiple distinct, scale-dependent links between fungi and decomposition. Ecol Lett 24:1352–1362. https://doi.org/10.1111/ele.13749

Stokland JN, Siitonen J, Jonsson BG (2012) Biodiversity in dead wood. Cambridge Univ. Press, Cambridge, UK

Thompson W, Rayner ADM (1982) Spatial structure of a population of *Tricholomopsis platyphylla* in a woodland site. New Phytol 92:103–114. https://doi.org/10.1111/j.1469-8137.1982.tb03366.x

Thompson W, Rayner ADM (1983) Extent, development and function of mycelial cord systems in soil. Trans Br Mycol Soc 81:333–345. https://doi.org/10.1016/S0007-1536(83)80085-0

Toljander YK, Lindahl BD, Holmer L, Högberg NOS (2006) Environmental fluctuations facilitate species co-existence and increase decomposition in communities of wood decay fungi. Oecologia 148:625–631. https://doi.org/10.1007/s00442-006-0406-3

Ulyshen MD, Wagner TL (2013) Quantifying arthropod contributions to wood decay. Methods Ecol Evol 4:345–352. https://doi.org/10.1111/2041-210x.12012

Vachaud G, Passerat De Silans A, Balabanis P, Vauclin M (1985) Temporal stability of spatially measured soil water probability density function. Soil Sci Soc Am J 49:822–828. https://doi.org/10.2136/sssaj1985.03615995004900040006x

van der Wal A, Ottosson E, de Boer W (2015) Neglected role of fungal community composition in explaining variation in wood decay rates. Ecology 96:124–133. https://doi.org/10.1890/14-0242.1

Vanderlinden K, Vereecken H, Hardelauf H et al (2012) Temporal stability of soil water contents: a review of data and analyses. Vadose Zone J 11(vzj2011):0178. https://doi.org/10.2136/vzj2011.0178

Waddell KL (2002) Sampling coarse woody debris for multiple attributes in extensive resource inventories. Ecol Ind 1:139–153. https://doi.org/10.1016/S1470-160X(01)00012-7

Wardle DA, Ghani A (1995) Why is the strength of relationships between pairs of methods for estimating soil microbial biomass often so variable? Soil Biol Biochem 27:821–828. https://doi.org/10.1016/0038-0717(94)00229-T

Weedon JT, Cornwell WK, Cornelissen JHC et al (2009) Global meta-analysis of wood decomposition rates: a role for trait variation among tree species? Ecol Lett 12:45–56. https://doi.org/10.1111/j.1461-0248.2008.01259.x

West AW, Sparling GP (1986) Modifications to the substrate-induced respiration method to permit measurement of microbial biomass in soils of differing water contents. J Microbiol Methods 5:177–189. https://doi.org/10.1016/0167-7012(86)90012-6

Wilson BT, Woodall CW, Griffith DM (2013) Imputing forest carbon stock estimates from inventory plots to a nationally continuous coverage. Carbon Balance Manag 8:1. https://doi.org/10.1186/1750-0680-8-1

Woodall CW, Monleon VJ (2008) Sampling protocol, estimation, and analysis procedures for the down woody materials indicator of the FIA Program. USDA Forest Service, Northern Research Station

Woodall CW, Walters BF, Oswalt SN et al (2013) Biomass and carbon attributes of downed woody materials in forests of the United States. For Ecol Manage 305:48–59. https://doi.org/10.1016/j.foreco.2013.05.030

Woodall CW, Fraver S, Oswalt SN et al (2021) Decadal dead wood biomass dynamics of coterminous US forests. Environ Res Lett 16:104034. https://doi.org/10.1088/1748-9326/ac29e8

Yin X (1999) The decay of forest woody debris: numerical modeling and implications based on some 300 data cases from North America. Oecologia 121:81–98. https://doi.org/10.1007/s004420050909

Zell J, Kändler G, Hanewinkel M (2009) Predicting constant decay rates of coarse woody debris—a meta-analysis approach with a mixed model. Ecol Model 220:904–912. https://doi.org/10.1016/j.ecolmodel.2009.01.020

Zhu J, Hu H, Tao S et al (2017) Carbon stocks and changes of dead organic matter in China's forests. Nat Commun 8:151. https://doi.org/10.1038/s41467-017-00207-1